

# Lipoyl-Based Antagonists of Transient Receptor Potential Cation A (TRPA1) Downregulate Osteosarcoma Cell Migration and Expression of Pro-Inflammatory Cytokines

Oscar Francesconi,<sup>▽</sup> Francisco Corzana,<sup>▽</sup> Georgia-Ioanna Kontogianni,<sup>▽</sup> Giorgio Pesciullesi, Roberta Guldani, Claudiu T. Supuran, Andrea Angeli, Rafaela Maria Kavasi, Maria Chatzinikolaidou,\* and Cristina Nativi\*

Cite This: *ACS Pharmacol. Transl. Sci.* 2022, 5, 1119–1127

Read Online

ACCESS |

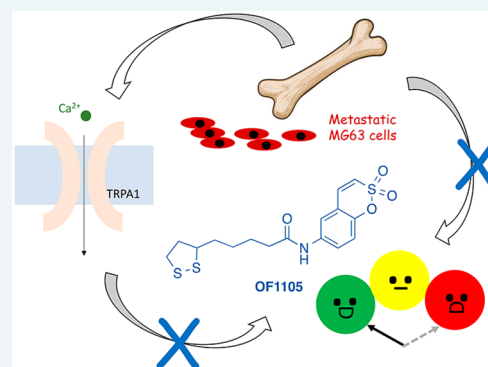
Metrics & More

Article Recommendations

Supporting Information

**ABSTRACT:** Osteosarcoma is a heterogeneous tumor intimately linked to its microenvironment, which promotes its growth and spread. It is generally accompanied by cancer-induced bone pain (CIBP), whose main component is neuropathic pain. The TRPA1 ion channel plays a key role in metastasis and is increasingly expressed in bone cancer. Here, a novel TRPA1 inhibitor is described and tested together with two other known TRPA1 antagonists. The novel lipoyl derivative has been successfully assessed for its ability to reduce human osteosarcoma MG-63 cell viability, motility, and gene expression of the CIBP pro-inflammatory cytokines interleukin 6 (IL-6) and tumor necrosis factor  $\alpha$  (TNF- $\alpha$ ). A putative three-dimensional (3D) model of the inhibitor covalently bound to TRPA1 is also proposed. The *in vitro* data suggest that the novel inhibitor described here may be highly interesting and stimulating for new strategies to treat osteosarcomas.

**KEYWORDS:** lipoyl derivatives, osteosarcoma, TRPA1 channel, neuropathic pain



The involvement of  $\text{Ca}^{2+}$ -permeable channels in several types of cancer is well known, and a direct correlation between their altered expression and cancer progression has extensively been reported.<sup>1</sup> Transient receptor potential (TRP) channels are  $\text{Ca}^{2+}$  channels involved in the regulation of many signalling pathways, including those related to carcinogenesis, tumor progression, and regulation of pain in cancer treatment.<sup>2</sup> Acute and chronic neuropathies associated with cancer and anticancer drug administration are indeed related to the remodelling and alteration in the expression of TRP  $\text{Ca}^{2+}$  channels. Moreover, a direct correlation between TRP channel expression and regulation of the motility of several cancer types has been reported.<sup>3</sup> In particular, in Lewis lung cancer cells, TRPM8 (melastatin 8) and TRPA1 (ankyrin-like 1) contribute to enhance cell detachment and promote metastasis.<sup>3</sup>

The TRPA1 channel is widely expressed in nociceptive neurons and a vast literature exists on ankyrin-like 1 as a chemosensor of noxious stimulus.<sup>4–6</sup> Albeit TRPA1 being also expressed in non-neuronal cells, like in lung epithelial fibroblasts, very little has been reported on its functions in malignancies. Recent evidence provided a rational basis on the implications of TRPA1 in lung adenocarcinoma, highlighting the binding of TRPA1 N-terminal ankyrin repeating units to the C-terminal membrane receptor fibroblast growth factor

receptor 2 (FGFR2). The TRPA1-FGFR2 interaction inhibits the channel, triggers the activation of the receptor, and promotes lung adenocarcinoma progression and metastasis. Downregulation of TRPA1 inhibits the TRPA1-mediated activation of FGFR2, hampering metastasis,<sup>7</sup> which is essential for hair-cell transduction.

Therefore, the emerging role of TRPA1 in metastasis,<sup>8–16</sup> the tendency of tumor cells originated in the lung to metastasize to the bone microenvironment,<sup>17</sup> and the amplification observed in bone cancer of the expression of TRPA1 in the dorsal root ganglion (DRG)<sup>17–19</sup> prompted us to study the effect of TRPA1 inhibition on the migration ability of osteosarcoma cells.

Osteosarcoma is a very heterogeneous tumor inextricably linked to its microenvironment, which is a fertile media for tumor cells to survive and growth.<sup>20</sup> Although advances in clinical management of osteosarcoma have progressed, the survival rates for patients with metastatic and recurrent disease

Received: June 12, 2022

Published: September 13, 2022



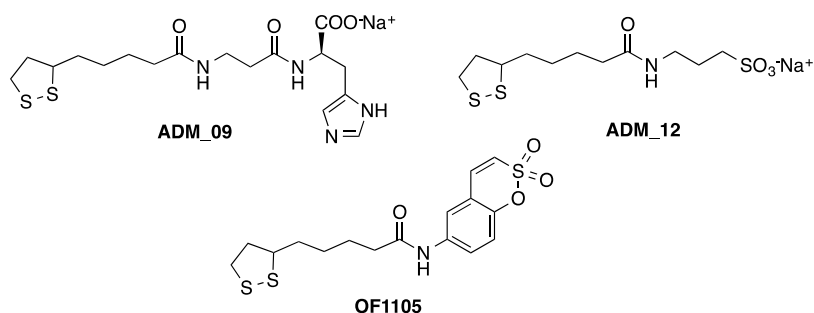


**Figure 1.** Structures of lipoyl derivatives ADM\_09, ADM\_12, and OF1105.

### Scheme 1. Synthesis of Lipoyl Derivative OF1105

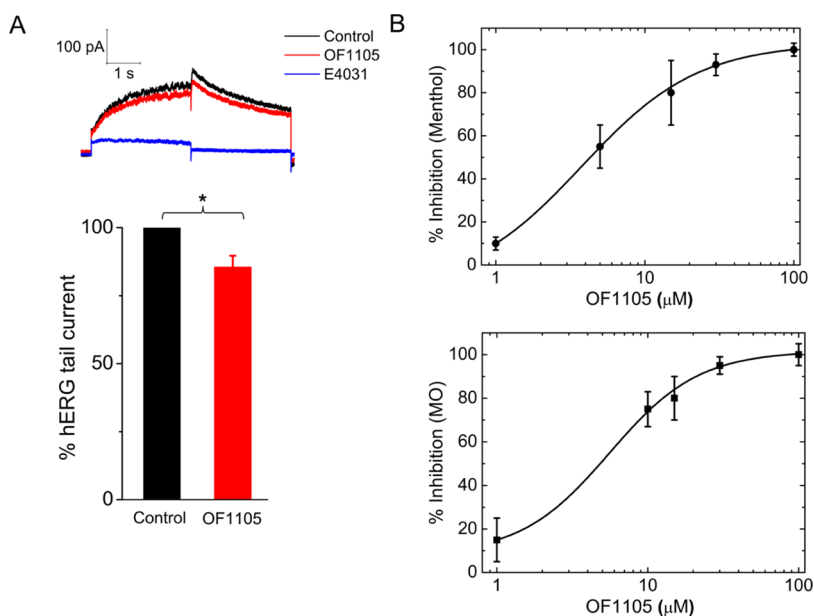
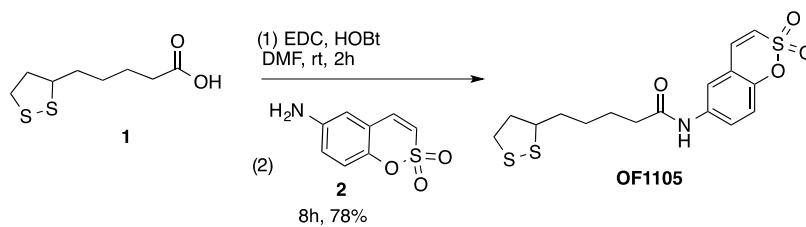


**Figure 2.** (A) (Top) Whole-cell currents (top) through hERG-HEK293 transfected cells under control conditions and in the presence of **OF1105** (1 mM) and **E4031** (100 nM). The reference compound **E4031** was tested at the end of each experiment to assess the contribution of endogenous currents. (Bottom) Mean relative tail-current amplitude before (control) and after application of 1 mM **OF1105**. Each column represents the mean  $\pm$  standard error of the mean (SEM) of  $n > 5$  cells. **OF1105** reduced the tail-current amplitude by  $15 \pm 4\%$ . (B) Dose-response curve (mean  $\pm$  SEM) obtained by patch clamp recordings through TRPA1-HEK293 transfected cells for the inhibition of 30  $\mu\text{M}$  menthol-induced currents (top), and 100  $\mu\text{M}$  MO-induced currents (bottom) by **OF1105** ( $n \geq 5$  per data point). The  $\text{IC}_{50}$  values obtained by fitting with a Hill equation are  $3.8 \pm 0.7 \mu\text{M}$  for menthol-induced currents, and  $5.6 \pm 1.9 \mu\text{M}$  for MO-induced currents.

remain below 20%.<sup>21</sup> Therefore, osteosarcoma treatment is still an urgent medical need.

Some years ago, we reported on two lipoyl derivatives, namely **ADM\_09**<sup>22</sup> and **ADM\_12**,<sup>23</sup> as TRPA1 antagonists able to revert the *in vivo* neuropathic pain induced by chemotherapy. Herein, we describe the synthesis of a new TRPA1 antagonist, namely **OF1105**, and report on the effects of **ADM\_09**, **ADM\_12**, and **OF1105** (Figure 1) on cancer bone cell viability, in reducing the migration of MG-63 osteosarcoma cells *in vitro*, and on gene expression levels of the pro-inflammatory cytokines IL-6 and TNF- $\alpha$  in MG-63.

Compounds **ADM\_09** and **ADM\_12** are effective antagonists of the nociceptive sensor channel TRPA1, whose persistent blocking effect has been proposed as the result of a synergistic combination of calcium-mediated binding of the polar hook and disulfide-bridge formation of the lipoyl acid residue.<sup>22</sup> Like **ADM\_09** and **ADM\_12**, the new derivative **OF1105** is a residue of lipoyl acid that is linked to a sulfocoumarin polar moiety through an amide bond (Figure 1). As previously reported,<sup>24</sup> sulfocoumarins may undergo enzymatic hydrolysis, unmasking a sulfonic acid residue

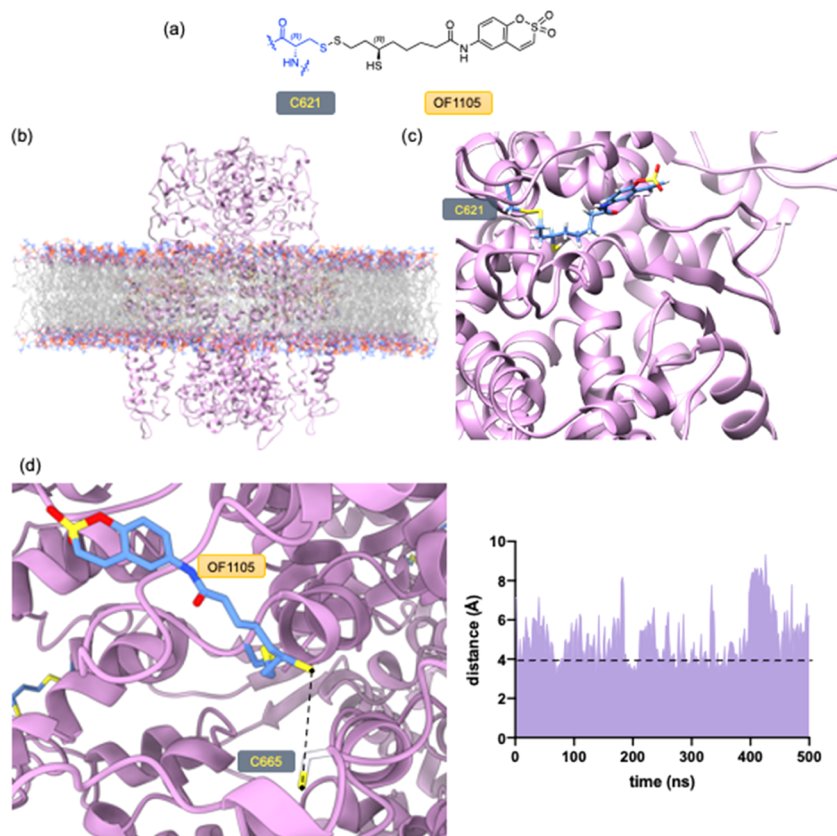


**Figure 3.** MD simulations of human TRPA1 ion channel in complex with the covalently bound OF1105 derivative and embedded in a lipid bilayer of 1,2-dioleoyl-*sn*-glycero-3-phosphocholine (DOPC). (a) Proposed structure for the complex upon the attack of Cys621 on OF1105. Only the conjugate with the (*R*) configuration at the new stereocenters is shown. (b) Model of TRPA1 and membrane interaction resulted from MD simulations. The membrane bilayer's apolar face is shown in light gray; phospholipids' external heads are shown in red, blue, and orange; and protein in purple. (c) A closer snapshot derived from 0.5  $\mu$ s MD simulations. Carbon atoms of the OF1105 derivative are shown in blue. (d) Monitoring the distance between the SH group in OF1105, formed upon reaction with the protein, and Cys665 by MD simulations. The atoms of the membrane, as well as solvent and ions, have been removed in (c) and (d) for clarity.

(Figure S1, Supporting Information) and making OF1105 an analogue of ADM<sub>12</sub>.

## RESULTS AND DISCUSSION

**Synthesis of the Lipoyl Derivative OF1105.** The synthesis of OF1105 was performed by activating the lipoic acid *in situ* with EDC and HOBt at room temperature and in dimethylformamide (DMF) as solvent, and adding to the reaction mixture the 6-amino sulfocoumarin 2.<sup>25</sup> The reaction was completed in 8 h and afforded after purification by column chromatography on silica gel the lipoyl amide OF1105 in good yield (78%) (Scheme 1).

As expected,<sup>26</sup> patch clamp experiments confirmed that OF1105 is an effective TRPA1 antagonist ( $IC_{50} = 3.8 \pm 0.7 \mu$ M for the inhibition of 30  $\mu$ M menthol-induced currents and  $5.6 \pm 1.9 \mu$ M for mustard oil (MO)-induced currents), while no inhibitory effect was recorded on hERG channels (no overt cardiotoxicity) (Figure 2 and Supporting Information).

**Molecular Dynamics Simulations.** To get insights into the binding interactions of the new lipoyl derivative, MD simulations were used to obtain a putative three-dimensional (3D) structure of the human TRPA1 ion channel in complex with the covalently bound OF1105 derivative and embedded in a lipid bilayer. For this purpose, we used the coordinates of TRPA1 obtained from the previously reported cryo-EM structure (PDB entry: 6pqp, see Methods for more details).<sup>27</sup>

First, the structure of OF1105 was superimposed on the structure of the human TRPA1 ion channel in complex with the covalent agonist benzyl isothiocyanate (BITC). As described previously,<sup>28</sup> we considered that compound OF1105 also reacts with Cys621, opening the 1,2-dithiolane ring. All possible complexes formed in this reaction were considered in the calculations (Figures 3a and S2). Interestingly, the complexes were stable throughout the simulations (see Figure 3b for the structure of the complex with the (*R*)-configuration at the new stereocenters generated upon the ring-opening reaction). In all complexes, the aromatic moiety was aligned and interacted hydrophobically with the lipid molecules, and only transient hydrogen bonding was detected throughout the trajectories, with populations <20% in all cases (Figure 3c). We also calculated by MD simulations the distance between the free remaining thiol group of OF1105, formed upon the reaction with the protein, and the remaining sulfhydryl groups of the Cys residues. According to our calculations, Cys665 showed on average ( $5.1 \pm 1.4 \text{ \AA}$ ) the lowest distance to the reactive SH center in OF1105 (Figure 3d). These data suggest that this Cys and the free SH of the lipoyl derivative may form an additional disulfide bond, as shown by us previously.<sup>22</sup> We have also tested this potential derivative by MD simulations for one of the isomers and found that the system is stable over the entire trajectory, with a root-

mean-square deviation (RMSD) value for the backbone atoms of 3.2 Å related to the cry-EM structure (see Figure S3).

**In Vitro Assessment. Cytotoxicity Assay.** At first, a cell viability assay was performed at a concentration of 100  $\mu\text{M}$  of the three inhibitors using normal human osteoblasts (NHOst). Previous studies on ADM\_09 and ADM\_12 have shown that the inhibitor at this concentration has high antioxidative properties (nitroblue tetrazolium test, NBT) and no toxicity (upon rat astrocytes).<sup>22,23</sup> Thus, the cells were seeded in 24-well plates ( $3 \times 10^4$  cells per well, day 0) and the inhibitors were added (day 1). Cell viability was measured after 1 and 2 days of incubation in the presence of the inhibitors. The results presented in Figure 4 demonstrate that both inhibitors

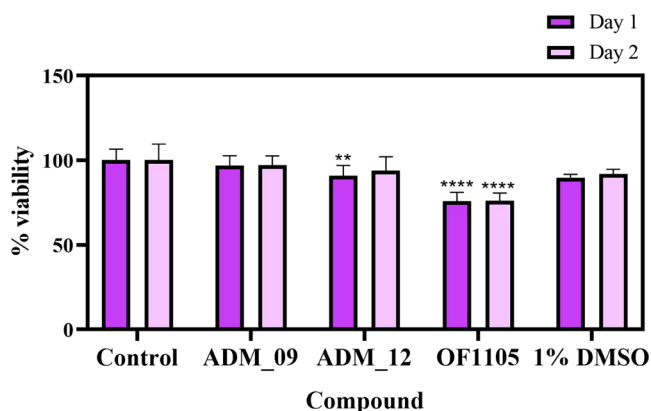


**Figure 4.** Cell viability assessment showing the viability of normal human osteoblasts (NHOst) and expressed as percent viability adjusted to the TCPS control for each experimental time point of 1 and 2 days in culture. Each bar represents the mean  $\pm$  standard deviation (SD) of quadruplicates in three independent experiments ( $n = 12$ ). Statistical analysis was performed for each compound (100  $\mu\text{M}$ ) and compared to the TCPS control at the same experimental time point (\*\* $p < 0.01$ , \*\*\*\* $p < 0.0001$ ).

ADM\_09 and ADM\_12 did not induce any cytotoxicity after 1 and 2 days of incubation, indicating cell viability values similar to those for the tissue culture polystyrene (TCPS) control surface, which are more than 90% of the control. For solubility reasons, OF1105 was dissolved in the organic solvent dimethyl sulfoxide (DMSO) and tested for its cytotoxic effects at a concentration of 100  $\mu\text{M}$ . A decrease of cell viability on days 1 and 2, reaching 75% of the viability compared to the TCPS control, was observed (see Supporting Information for details). In order to assess if the cytotoxic effect of OF1105 is due to its pre-dilution in 1% DMSO, an extra control was tested. DMSO was dissolved in culture medium at the same concentration used for the OF1105 dissolution, and the cell viability assay was performed in NHOst cells. As shown in Figure 4, 1% DMSO does not indicate any cytotoxic effect and displays similar cell viability levels compared to the control culture.

To detect possible differences of the tested molecules between normal and cancer cells, cytotoxicity was also evaluated in MG-63 human osteosarcoma cells. The protocol, as above reported for NHOst, was followed. The results presented in Figure 5 show a high cell viability for both ADM\_09 and ADM\_12, similar to the TCPS control. Conversely, the incubation of MG-63 cells with OF1105 induced a decreasing cell viability compared to the control, of 35 and 29% after 1 and 2 days of incubation, respectively

(Figure 5). DMSO as control has comparable cell viability values with the control culture; therefore, the decreased cell

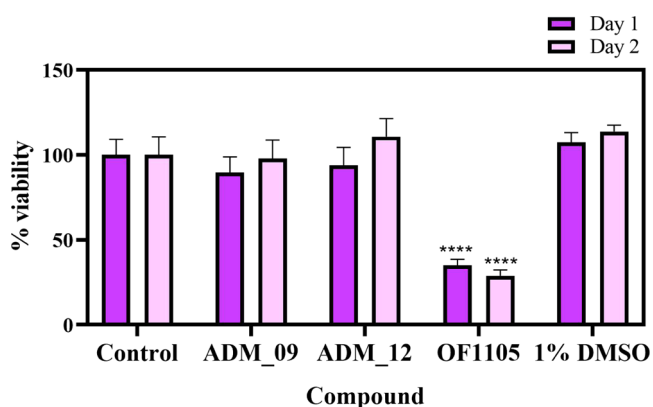


**Figure 5.** Cell viability assessment showing the viability of MG-63 human osteosarcoma cells expressed as percent viability adjusted at 100% of the TCPS control for each time point of 1 and 2 days in culture. Each bar represents the mean  $\pm$  SD of quadruplicates in three independent experiments ( $n = 12$ ). Statistical analysis was performed for each compound (100  $\mu\text{M}$ ) and compared to the TCPS control at the same experimental time point (\*\*\*\* $p < 0.0001$ ).

viability of OF1105 is due to the presence of the tested inhibitor and not because of the organic solvent. These results indicate that OF1105 has a higher cytotoxic effect on MG-63 osteosarcoma cells in comparison with the physiological cell type, such as the normal human osteoblasts.

Trying to rationalize these data, we considered previous studies<sup>24</sup> reporting on the cytotoxicity of ADM\_12 in human colon cancer cells HT-29 ascribed to the inhibition of carbonic anhydrases (CAs) IX and XII, a superfamily of zinc metalloenzymes involved in many types of cancer progression. Assuming that in a tumoral microenvironment OF1105 might undergo the sulfocoumarin ring opening (see above),<sup>23</sup> we investigated its possible CA inhibition properties. However, OF1105 showed a poor (micromolar range) inhibition of human CAIX and CAXII, sensibly lower than that reported for ADM\_12 (see Table S3, Supporting Information). The low inhibition observed suggests a scarce interaction of OF1105 with CAs' binding site, likely due to a poorly accessible sulfonate group, which in OF1105 likely does not undergo hydrolysis to sulfonic acid.

**Wound Healing Assay.** Cell migration is a central component of the metastatic cascade requiring a concerted action of ion channels and transporters. The ion transport protein's role in tumor cell migration and invasion includes the induction of local volume changes and/or modulation of  $\text{Ca}^{2+}$ ,  $\text{K}^+$ , and  $\text{H}^+$  signalling. Ion transport proteins, including the TRP channel superfamily, are considered attractive candidate targets for the reduction of cancer migration because, as membrane proteins, they are easily accessible and often overexpressed or activated in cancer.<sup>29,30</sup> Therefore, the highly aggressive MG-63 human osteosarcoma cells were used in a wound healing model to evaluate the possible effects of ADM\_09, ADM\_12, and OF1105 on the ability of osteosarcoma cells to migrate, thus reflecting their effect on the metastatic activity of osteosarcoma cells. The results show that in control samples (cells only) the closure was approximately 20%, as expected according to the literature.<sup>31,32</sup> Interestingly, the TRPA1 inhibitors slowed down the migration

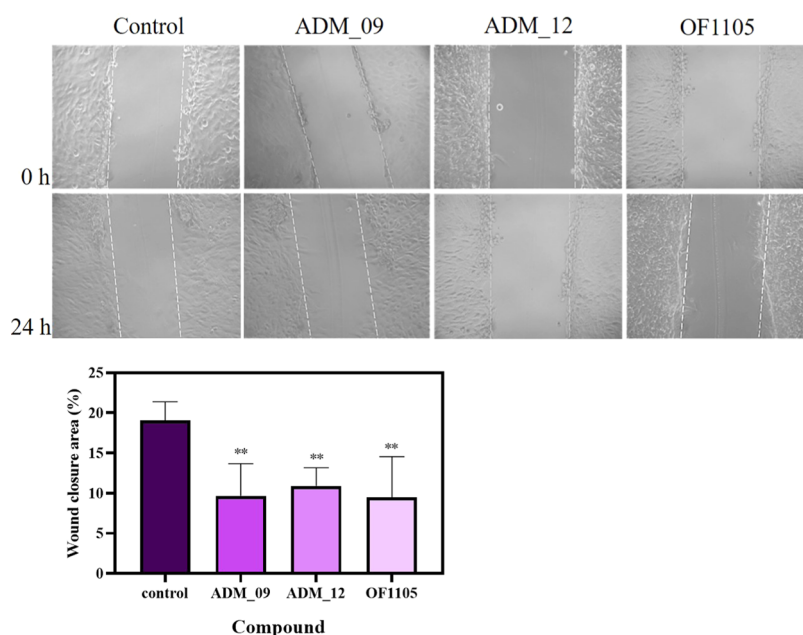


**Figure 6.** Migration assay on MG-63 human osteosarcoma cells. After serum starvation for 24 h, the inhibitors ADM\_09, ADM\_12, and OF1105 were added at a concentration of 100  $\mu$ M in 0% DMEM and a wound was created with a 10  $\mu$ L sterile tip. Upper panel: micrographs were taken at a 10-fold magnification at 0 and 24 h. Lower panel: the graph represents the percent wound closure area. Statistical analysis indicates the differences between each compound compared to the control (\*\* $p < 0.01$ ).

rate, as the wound closure was approximately 10% for all of them. Hence, our results indicate that the TRPA1 channel plays a role in the metastatic capacity of osteosarcoma, and the addition of the inhibitors ADM\_09, ADM\_12, and OF1105 resulted in a significant downregulation of the MG-63 cell migration (Figure 6). The antimetastatic capacities of ADM\_09, ADM\_12, and OF1105 reported herein agree with previous reports indicating that alterations and blocking in the ion transport proteins lead to a reduction in the migration ability of tumor cells.<sup>33</sup> In particular, it has been recognized that  $\text{Ca}^{2+}$  signals have regulatory effects on cell motility since they target contractile proteins and many regulatory proteins.<sup>34,35</sup>

**Expression of the TRPA1 Receptor in MG-63 Cells and Gene Expression of the Inflammatory Markers IL-6 and TNF- $\alpha$ .** Pain caused by bone metastasis (cancer-induced bone pain (CIBP)) is an important factor affecting the quality of life of oncologic patients. Currently, it is suggested that neuropathic pain is a main component of CIBP.<sup>28</sup> The pathways of neuropathic pain are not well understood. Neuropathic pain is a complex phenomenon caused by interactions between multiple physiological systems, including the immune system. Based on the current evidence, both pro- and anti-inflammatory cytokines appear to play an important role in the development of neuropathic pain; on the other hand, the relevant involvement of TRPA1 in different patterns of neuropathic pain is worldwide accepted. IL-6 and TNF- $\alpha$  are pro-inflammatory cytokines that play a crucial role in the development and maintenance of inflammatory pain and can induce pain through the release of inflammatory mediators sensitizing ion channels.<sup>15</sup> TRP transcripts are accompanied by increased IL-6 and TNF- $\alpha$  mRNA levels, and it is known that the TRPA1 channel can be sensitized by inflammatory agents causing its upregulation.<sup>36,37</sup> Previous studies have shown that inhibition of either IL-6 or TNF- $\alpha$  expression attenuated the

expression of TRPA1, reducing the mechanical hyperalgesia and thermal hypersensitivity induced by bone cancer.<sup>17</sup>

At first, we examined if the MG-63 cells express the TRPA1 receptor. RNA was extracted from an untreated cell culture and reverse transcribed. In the synthesized cDNA, polymerase chain reaction (PCR) was performed with specific primers for TRPA1. Figure 7 presents the results of the PCR for the untreated cells (control culture) and confirms the expression of TRPA1 receptor in MG-63 cells.

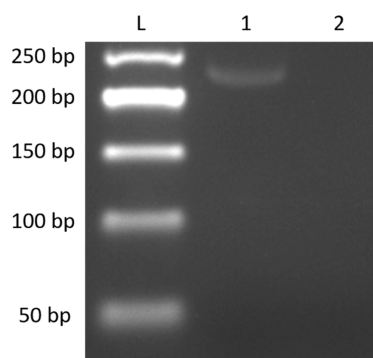


**Figure 7.** Agarose gel electrophoresis for the amplified TRPA1 receptor in a control culture of MG-63 cells and visualization under ultraviolet (UV) light after staining with gel red (L: ladder, 1: positive control, 2: negative control).

Thus, RNA extraction of MG-63 cells treated with ADM\_09, ADM\_12, and OF1105 was performed after 1, 2, and 3 days of culture to examine the gene expression levels of IL-6 and TNF- $\alpha$  in osteosarcoma cells treated with the three inhibitors and with respect to a control cell culture (Figure 8).

The levels of IL-6 mRNA expression of MG-63 cells were significantly decreased after the treatment with ADM\_09 after 1 and 2 days of incubation, with a significant increase on day 3

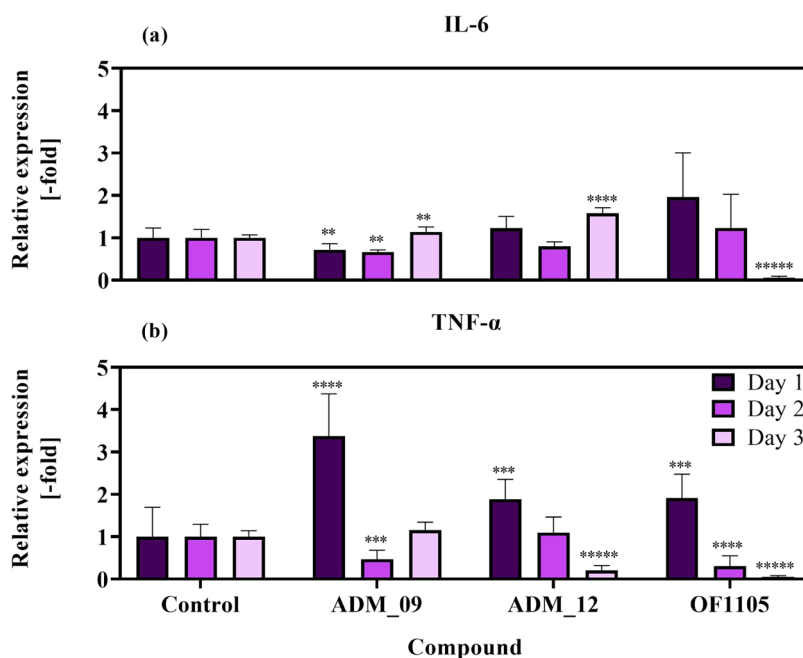


**Figure 8.** Real-time PCR analysis of the expression of pro-inflammatory cytokines including IL-6 (a) and TNF- $\alpha$  (b) in MG-63 osteosarcoma cells seeded with and without ADM\_09, ADM\_12, and OF1105 after 1, 2, and 3 days of culture. The values present means  $\pm$  SD of triplicates in three independent experiments ( $n = 9$ ). B2M and GAPDH were used as housekeeping genes. Statistical analysis was performed for each compound (100  $\mu$ M) and compared to the TCPS control at the same experimental time point (\*\* $p < 0.001$ , \*\*\*\* $p < 0.0001$ , \*\*\*\*\* $p < 0.00001$ ).

(Figure 8a). On the contrary, TNF- $\alpha$  showed a significant upregulation on day 1 followed by an approximately 3-fold reduction on day 2 (Figure 8b). ADM\_12 administration caused an upregulation of IL-6 mRNA expression levels after 3 days of culture in comparison with the control culture (Figure 8a), while the TNF- $\alpha$  expression levels showed a significant increase after day 1, followed by a significant decrease after 3 days in culture (Figure 8b). The latter agrees with a report on *in vivo* experiments indicating that systemic administration of ADM\_12 reduced the mRNA levels of both cytokines.<sup>19</sup> Notably, the cells' treatment with OF1105 indicates a remarkable downregulation of both inflammatory cytokines IL-6 and TNF- $\alpha$  after 3 days in culture compared to the nontreated control.

## CONCLUSIONS

In the current study, the synthesis of the new lipoyl derivative OF1105 is described. The compound OF1105 is structurally related to the TRPA1 inhibitors ADM\_09 and ADM\_12 we previously reported. The inhibition properties of OF1105 vs TRPA1 have been assessed and tentatively rationalized by MD simulations relying on coordinates of human TRPA1 obtained from the cryo-EM structure previously reported.<sup>27</sup> Indeed, OF1105 could undergo a ring-opening reaction through the 1,2-dithiolane moiety with Cys621 to form a covalently linked complex (Figure 3). According to our MD simulations, the resulting conjugate is stable throughout the simulation time and OF1105 is engaged in transient hydrogen bonds with the protein. Of note, the simulations also show that Cys665 is close enough to form an additional disulfide bond with the remaining -SH group of OF1105.

Cytotoxicity tests performed on ADM\_09, ADM\_12, and OF1105 using normal human osteoblast (NHOst) (see Figure 4) and human osteosarcoma MG-63 (see Figure 4) cells indicated similar cell viabilities for ADM\_09 and ADM\_12 as

the control culture (no reduction after 1 and 2 days of incubation). For OF1105, even though a moderate decrease of viability of NHOst cells (up to 25%) was recorded, a remarkable reduction of MG-63 viability was assessed (65%, day 1 and 71%, day 2). The effects of ADM\_09, ADM\_12, and OF1105 on the ability of aggressive MG-63 cells to migrate and colonize tissues were evaluated using a wound healing model. Each of the three compounds slowed down the cell migration rate, with a reduction of wound closure from 20% (cells only as control) to 10% (Figure 6). Additionally, the gene therapy strategy that relieves neuropathic pain by silencing TNF- $\alpha$  expression in DRG using the RNA interference technology with lentiviral vectors showed that TNF- $\alpha$  and IL-6 expression levels were significantly reduced after 3 days of administration of each of the three inhibitors in comparison with the control culture.<sup>38</sup> Our results on the downregulation of the TNF- $\alpha$  and IL-6 gene expression (see Figure 8) are in line with the reported findings. These data prove the ability of the three compounds in reverting the expression of pro-inflammatory cytokines and presumably reducing neuropathic pain through the downregulation of TRPA1, in agreement with previous reports on the ability of ADM\_09 and ADM\_12 to counteract "*in vivo*" neuropathic pain.<sup>19,23</sup> Assuming for OF1105 the same mechanism of action as ADM\_09 and ADM\_12, it was expected to observe similar trends for the three compounds in terms of cell viability and migration. Surprisingly, the new lipoyl derivative caused a significant reduction of osteosarcoma cells' MG-63 viability and a striking downregulation of both TNF- $\alpha$  and IL-6 pro-inflammatory cytokines (on day 3), proving it as the most promising among the three compounds investigated.

Concluding, herein we reported on the beneficial role of TRPA1 inhibitors in regulating osteosarcoma cell migration and in reducing the level of inflammatory markers IL-6 and TNF- $\alpha$ , known to trigger CIBP. It is worthy of noting that,

albeit a rational basis on the implication of TRPA1 in lung adenocarcinoma has been provided, unprecedentedly, our results demonstrate that TRPA1 inhibitors are also involved in osteosarcoma cell motility. Since lung adenocarcinomas tend to form metastases in bones, these results are of high interest and the inhibitor OF1105 herein reported might be of inspiration for new strategies to treat osteosarcomas and the still intractable CIBP.

## EXPERIMENTAL SECTION

**General Methods.** High-grade reagents and solvents were purchased from commercial suppliers and were used without further purification. Reactions were followed by analytical thin-layer chromatography (TLC plates, Merck silica gel 60 F254), and compounds were detected under UV light ( $\lambda = 254$  or  $365$  nm) and/or stained with 10 wt % phosphomolybdic acid solution in EtOH.

**Synthesis of Lipoyl Derivative OF1105.** To a solution of lipoic acid (230 mg, 1.12 mmol) in 12 mL of DMF, EDAC HCl (429 mg, 2.24 mmol) and 1-hydroxybenzotriazole hydrate (242 mg, 1.79 mmol) were added. The solution was stirred for 1 h; then 6-amino sulfocoumarin (220 mg, 1.12 mmol) was added and the solution stirred overnight at room temperature. The reaction mixture was diluted with ethyl acetate (300 mL) and washed twice with a solution of citric acid (10%), twice with  $\text{NaHCO}_3$  s.s., and then twice with water. After removal of the solvent under vacuum, 400 mg of a crude sample was obtained. The crude sample was purified by flash chromatography on silica gel (5% methanol in dichloromethane) to obtain 338 mg of pure OF1105 (0.877 mmol, 78%) as a pale-yellow powder.  $M_p$ :  $> 245$  °C (dec).  $^1\text{H}$  NMR ( $\text{DMSO-}d_6$ , 500 MHz):  $\delta$  10.17 (s, 1H), 8.02 (d,  $J = 2.88$  Hz, 1H), 7.72 (d,  $J = 10.08$  Hz, 1H), 7.62 (dd,  $J = 9.12$  Hz,  $J = 2.88$  Hz, 1H), 7.50 (d,  $J = 10.08$  Hz, 1H), 7.39 (d,  $J = 9.12$  Hz, 1H), 3.67–3.61 (m, 1H), 3.22–3.18 (m, 1H), 3.17–3.10 (m, 1H), 2.46–2.39 (m, 1H), 2.34 (t,  $J = 6.72$  Hz, 2H), 1.92–1.85 (m, 1H), 1.73–1.55 (m, 4H), 1.45–1.39 (m, 2H).  $^{13}\text{C}\{^1\text{H}\}$  NMR ( $\text{CDCl}_3$ , 125 MHz): 171.24, 147.39, 135.90, 135.82, 122.97, 122.76, 120.14, 119.29, 119.28, 56.38, 40.29, 38.51, 37.27, 34.59, 28.79, 25.06. HRMS  $m/z$ :  $[\text{M} + \text{H}]^+$  Calcd for  $\text{C}_{16}\text{H}_{20}\text{O}_4\text{NS}_3$ , 386.0549; found 386.0547.

**CA Inhibition Assay.** An Applied Photophysics stopped-flow instrument was used to assay the CA-catalyzed  $\text{CO}_2$  hydration activity.<sup>24,25</sup> Phenol red (at a concentration of 0.2 mM) was used as an indicator, working at the absorbance maximum of 557 nm, with 20 mM Hepes (pH 7.4) as a buffer, and 20 mM  $\text{Na}_2\text{SO}_4$  (to maintain constant ionic strength), following the initial rates of the CA-catalyzed  $\text{CO}_2$  hydration reaction for a period of 10–100 s. The  $\text{CO}_2$  concentrations ranged from 1.7 to 17 mM for the determination of the kinetic parameters and inhibition constants. Enzyme concentrations ranged between 5 and 12 nM. For each inhibitor, at least six traces of the initial 5–10% of the reaction were used to determine the initial velocity. The uncatalyzed rates were determined in the same manner and subtracted from the total observed rates. Stock solutions of the inhibitor (0.1 mM) were prepared in distilled–deionized water and dilutions up to 0.01 nM were done thereafter with the assay buffer. Inhibitor and enzyme solutions were preincubated together for 15 min at room temperature prior to the assay, to allow for the formation of the E–I complex. The inhibition constants were obtained by nonlinear least-squares methods using PRISM 3 and the Cheng–Prusoff equation as reported earlier and represent the

mean from at least three different determinations. All CA isoforms were recombinant proteins obtained in-house, as reported earlier.<sup>25</sup>

**Cell Viability Assessment.** The viability and proliferation of both cell types NHOst and MG-63 were assessed using the PrestoBlue viability assay (Invitrogen Life Technologies).<sup>39</sup> When cells retain their viability, they maintain a reducing environment within their cytosol. The nontoxic metabolic indicator resazurin is modified by the reducing environment; it becomes red, and can be detected photometrically. For the viability experiments,  $3 \times 10^4$  cells/well were seeded on day 0 and cell viability was measured after 1 and 2 days in culture. Absorbance measurements related to cell viability were performed using a spectrophotometer (Synergy HTX Multi-Mode Microplate Reader, BioTek, Winooski, VT) at 570 and 600 nm. Experiments were performed in quadruplicates in three independent experiments ( $n = 12$ ). In all experiments, tissue culture polystyrene (TCPS) was used as the control surface in cell culture.

**Culture of Human Osteosarcoma Cells MG-63.** Osteosarcoma cells MG-63 provided by Sigma (86051601) were cultured in DMEM supplemented with 10% (v/v) FBS, 100  $\mu\text{g}/\text{mL}$  penicillin and streptomycin (PAN-Biotech, Germany), 2 mM L-glutamine (PAN-Biotech, Germany), and 2.5  $\mu\text{g}/\text{mL}$  Amphotericin (Gibco, Thermo Fisher Scientific, U.K.) in a humidified incubator at 37 °C in 5%  $\text{CO}_2$ . The culture medium was replaced twice weekly. The cells were detached using trypsin-0.25% EDTA. For the cell viability experiments,  $3 \times 10^4$  cells were seeded per well in 24-well plates, while  $8 \times 10^4$  cells per well were cultured in 24-well plates for the real-time quantitative polymerase chain reaction (PCR) experiments.

**Wound Healing Assay.** The wound healing assay was performed as previously described.<sup>32</sup> MG-63 cells were seeded in 24-well plates at a concentration of  $6 \times 10^4$  cells per well on day 0. The optimal concentration for plating was selected so that the cells would be confluent after 72 h of incubation at 37 °C and 5%  $\text{CO}_2$ . After serum starvation for 24 h (using Dulbecco's Modified Eagle Medium, DMEM, 0% FBS culture medium), the inhibitors were added at a concentration of 100  $\mu\text{M}$  diluted in DMEM 0% medium and the cells were incubated for 24 h. On day 3, the confluent cell layer was wounded by scratching it with a sterile 10  $\mu\text{L}$  pipette tip. Photographs were taken at 0 and 24 h by means of a Zeiss Axiovert 200 microscope at a 10-fold magnification, and the wound closure was analyzed by means of Image J software.

## ASSOCIATED CONTENT

### Supporting Information

The Supporting Information is available free of charge at <https://pubs.acs.org/doi/10.1021/acspsci.2c00114>.

Molecular modelling data; patch clamp measurements; in vitro tests methods and materials; gene expression; polymerase chain reaction, and CAs inhibition tests assessment (PDF)

## AUTHOR INFORMATION

### Corresponding Authors

Maria Chatzinikolaidou – Department of Materials Science and Technology, University of Crete, 70013 Heraklion, Greece; Foundation for Research and Technology Hellas (FORTH), Institute of Electronic Structure and Laser

(IESL), 70013 Heraklion, Greece; Phone: +30 2810394276; Email: [mchatzin@materials.uoc.gr](mailto:mchatzin@materials.uoc.gr)  
Cristina Nativi – Department of Chemistry, DICUS, University of Florence, 50019 Florence, Italy; [orcid.org/0000-0002-6312-3230](https://orcid.org/0000-0002-6312-3230); Phone: +39 0554573540; Email: [cristina.nativi@unifi.it](mailto:cristina.nativi@unifi.it)

## Authors

Oscar Francesconi – Department of Chemistry, DICUS, University of Florence, 50019 Florence, Italy; [orcid.org/0000-0002-6155-4926](https://orcid.org/0000-0002-6155-4926)  
Francisco Corzana – Departamento de Química, Centro de Investigación en Síntesis Química, Universidad de La Rioja, 26006 Logroño, Spain; [orcid.org/0000-0001-5597-8127](https://orcid.org/0000-0001-5597-8127)  
Georgia-Ioanna Kontogianni – Department of Materials Science and Technology, University of Crete, 70013 Heraklion, Greece  
Giorgio Pesciullesi – Department of Chemistry, DICUS, University of Florence, 50019 Florence, Italy  
Roberta Galdani – Department of Chemistry, DICUS, University of Florence, 50019 Florence, Italy; Present Address: Institute of Neuroscience, Université catholique de Louvain, B-1200 Brussels, Belgium; [orcid.org/0000-0003-3617-4953](https://orcid.org/0000-0003-3617-4953)  
Claudiu T. Supuran – NEUROFARBA Department, Sezione di Scienze Farmaceutiche, University of Florence, 50019 Florence, Italy; [orcid.org/0000-0003-4262-0323](https://orcid.org/0000-0003-4262-0323)  
Andrea Angeli – NEUROFARBA Department, Sezione di Scienze Farmaceutiche, University of Florence, 50019 Florence, Italy; [orcid.org/0000-0002-1470-7192](https://orcid.org/0000-0002-1470-7192)  
Rafaella Maria Kavasi – Foundation for Research and Technology Hellas (FORTH), Institute of Electronic Structure and Laser (IESL), 70013 Heraklion, Greece

Complete contact information is available at:  
<https://pubs.acs.org/10.1021/acspstsci.2c00114>

## Author Contributions

<sup>∇</sup>O.F., F.C., and G.-I.K. contributed equally to this work and co-first authorship. The manuscript was written through the contributions of O.F., F.C., G.-I.K., R.-M.K., M.C., and C.N. All authors have given approval to the final version of the manuscript.

## Funding

COST Action “Functional Glycomaterials for the Developments of Diagnostic and Targeted Therapeutic Probes - GlycoNanoProbes” CM18132, Fondazione Cassa di Risparmio Firenze; European Union’s Horizon 2020 research and innovation program (grant agreement No 814410), Agencia Estatal Investigación of Spain (AEI; Grant RTI2018-099592-B-C21).

## Notes

The authors declare no competing financial interest.

## ACKNOWLEDGMENTS

The authors thank COST Action “GlycoNanoProbes” CM18132. Fondazione Cassa di Risparmio Firenze and the European Union’s Horizon 2020 research and innovation program under grant agreement no. 814410 are acknowledged for financial support. F.C. thanks the Agencia Estatal Investigación of Spain (AEI; Grant RTI2018-099592-B-C21).

## ABBREVIATIONS

TRP, transient receptor potential; FGFR2, fibroblast growth factor receptor 2; MD, molecular dynamic; NHO, normal human osteoblast; TCPS, tissue culture polystyrene; CA, carbonic anhydrase; TLC, thin-layer chromatography

## REFERENCES

- (1) Chinigò, G.; Pla, A. F.; Gkika, D. TRP Channels and Small GTPases Interplay in the Main Hallmarks of Metastatic Cancer. *Front. Pharmacol.* **2020**, *11*, No. 581455.
- (2) Shapovalov, G.; Ritaine, A.; Skryma, R.; Prevarskaya, N. Role of TRP Ion Channels in Cancer and Tumorigenesis. *Semin. Immunopathol.* **2016**, 357–369.
- (3) Du, G. J.; Li, J. H.; Liu, W. J.; Liu, Y. H.; Zhao, B.; Li, H. R.; Hou, X. D.; Li, H.; Qi, X. X.; Duan, Y. J. The Combination of TRPM8 and TRPA1 Expression Causes an Invasive Phenotype in Lung Cancer. *Tumor Biol.* **2014**, *35*, 1251–1261.
- (4) Koivisto, A.; Jalava, N.; Bratty, R.; Pertovaara, A. TRPA1 Antagonists for Pain Relief. *Pharmaceuticals* **2018**, *11*, No. 117.
- (5) Chen, Y.; Li, G.; Huang, L. Y. M. P2X7 Receptors in Satellite Glial Cells Mediate High Functional Expression of P2X3 Receptors in Immature Dorsal Root Ganglion Neurons. *Mol. Pain* **2012**, *8*, 1744–8069.
- (6) Nassini, R.; Gees, M.; Harrison, S.; De Siena, G.; Materazzi, S.; Moretto, N.; Failli, P.; Preti, D.; Marchetti, N.; Cavazzini, A.; Mancini, F.; Pedretti, P.; Nilius, B.; Patacchini, R.; Geppetti, P. Oxaliplatin Elicits Mechanical and Cold Allodynia in Rodents via TRPA1 Receptor Stimulation. *Pain* **2011**, *152*, 1621–1631.
- (7) Berrout, J.; Kyriakopoulou, E.; Moparthi, L.; Hogeia, A. S.; Berrout, L.; Ivan, C.; Lorget, M.; Boyle, J.; Peers, C.; Muench, S.; Gomez, J. E.; Hu, X.; Hurst, C.; Hall, T.; Umamaheswaran, S.; Wesley, L.; Gagea, M.; Shires, M.; Manfield, I.; Knowles, M. A.; Davies, S.; Suhling, K.; Gonzalez, Y. T.; Carragher, N.; Macleod, K.; Abbott, N. J.; Calin, G. A.; Gamper, N.; Zygmunt, P. M.; Timsah, Z. TRPA1-FGFR2 Binding Event Is a Regulatory Oncogenic Driver Modulated by MiRNA-142-3p. *Nat. Commun.* **2017**, *8*, No. 947.
- (8) Malsch, P.; Andratsch, M.; Vogl, C.; Link, A. S.; Alzheimer, C.; Brierley, S. M.; Hughes, P. A.; Kress, M. Deletion of Interleukin-6 Signal Transducer Gp130 in Small Sensory Neurons Attenuates Mechanonociception and down-Regulates TRPA1 Expression. *J. Neurosci.* **2014**, *34*, 9845–9856.
- (9) Manjavachi, M. N.; Motta, E. M.; Marotta, D. M.; Leite, D. F. P.; Calixto, J. B. Mechanisms Involved in IL-6-Induced Muscular Mechanical Hyperalgesia in Mice. *Pain* **2010**, *151*, 345–355.
- (10) el Karim, I.; McCrudden, M. T. C.; Linden, G. J.; Abdullah, H.; Curtis, T. M.; McGahon, M.; About, I.; Irwin, C.; Lundy, F. T. TNF- $\alpha$ -Induced P38MAPK Activation Regulates TRPA1 and TRPV4 Activity in Odontoblast-like Cells. *Am. J. Pathol.* **2015**, *185*, 2994–3002.
- (11) Jin, X.; Gereau, R. W., IV Acute P38-Mediated Modulation of Tetrodotoxin-Resistant Sodium Channels in Mouse Sensory Neurons by Tumor Necrosis Factor- $\alpha$ . *J. Neurosci.* **2006**, *26*, 246–255.
- (12) Marchand, F.; Perretti, M.; McMahon, S. B. Role of the Immune System in Chronic Pain. *Nat. Rev. Neurosci.* **2005**, *6*, 521–532.
- (13) Lees, J. G.; Makker, P. G. S.; Tonkin, R. S.; Abdulla, M.; Park, S. B.; Goldstein, D.; Moalem-Taylor, G. Immune-Mediated Processes Implicated in Chemotherapy-Induced Peripheral Neuropathy. *Eur. J. Cancer* **2017**, *73*, 22–29.
- (14) Gwak, Y. S.; Hulsebosch, C. E.; Leem, J. W. Neuronal-Glial Interactions Maintain Chronic Neuropathic Pain after Spinal Cord Injury. *Neural Plast.* **2017**, 2017, 1–14.
- (15) Miller, R. J.; Jung, H.; Bhangoo, S. K.; White, F. A. Cytokine and Chemokine Regulation of Sensory Neuron Function. *Sens. Nerves* **2009**, 417–449.
- (16) Skaper, S. D.; Facci, L.; Zusso, M.; Giusti, P. Neuroinflammation, Mast Cells, and Glia: Dangerous Liaisons. *Neuroscientist* **2017**, *23*, 478–498.



(17) Zhao, D.; Han, D. F.; Wang, S. S.; Lv, B.; Wang, X.; Ma, C. Roles of Tumor Necrosis Factor- $\alpha$  and Interleukin-6 in Regulating Bone Cancer Pain via TRPA1 Signal Pathway and Beneficial Effects of Inhibition of Neuro-Inflammation and TRPA1. *Mol. Pain* **2019**, *15*, No. 174480691985798.

(18) Demartini, C.; Tassorelli, C.; Zanaboni, A. M.; Tonsi, G.; Francesconi, O.; Nativi, C.; Greco, R. The Role of the Transient Receptor Potential Ankyrin Type-1 (TRPA1) Channel in Migraine Pain: Evaluation in an Animal Model. *J. Headache Pain* **2017**, *18*, No. 94.

(19) Demartini, C.; Greco, R.; Zanaboni, A. M.; Francesconi, O.; Nativi, C.; Tassorelli, C.; Deseure, K. Antagonism of Transient Receptor Potential Ankyrin Type-1 Channels as a Potential Target for the Treatment of Trigeminal Neuropathic Pain: Study in an Animal Model. *Int. J. Mol. Sci.* **2018**, *19*, No. 3320.

(20) Corre, I.; Verrecchia, F.; Crenn, V.; Redini, F.; Trichet, V. The Osteosarcoma Microenvironment: A Complex But Targetable Ecosystem. *Cells* **2020**, *9*, No. 976.

(21) Abarrategi, A.; Tornin, J.; Martinez-Cruzado, L.; Hamilton, A.; Martinez-Campos, E.; Rodrigo, J. P.; González, M. V.; Baldini, N.; Garcia-Castro, J.; Rodriguez, R. Osteosarcoma: Cells-of-Origin, Cancer Stem Cells, and Targeted Therapies. *Stem Cells Int.* **2016**, *2016*, 1–13.

(22) Nativi, C.; Gualdani, R.; Dragoni, E.; Di Cesare Mannelli, L.; Sostegni, S.; Norcini, M.; Gabrielli, G.; la Marca, G.; Richichi, B.; Francesconi, O.; Moncelli, M. R.; Ghelardini, C.; Roelens, S. A TRPA1 Antagonist Reverts Oxaliplatin-Induced Neuropathic Pain. *Sci. Rep.* **2013**, *3*, No. 2005.

(23) Gualdani, R.; Ceruti, S.; Magni, G.; Merli, D.; Di Cesare Mannelli, L.; Francesconi, O.; Richichi, B.; la Marca, G.; Ghelardini, C.; Moncelli, M. R.; Nativi, C. Lipoic-Based TRPA1/TRPV1 Antagonist to Treat Orofacial Pain. *ACS Chem. Neurosci.* **2015**, *6*, 380–385.

(24) Fragai, M.; Comito, G.; Di Cesare Mannelli, L.; Gualdani, R.; Calderone, V.; Louka, A.; Richichi, B.; Francesconi, O.; Angeli, A.; Nocentini, A.; Gratteri, P.; Chiarugi, P.; Ghelardini, C.; Tadini-Buoninsegni, F.; Supuran, C. T.; Nativi, C. Lipoyl-Homotaurine Derivative (ADM-12) Reverts Oxaliplatin-Induced Neuropathy and Reduces Cancer Cells Malignancy by Inhibiting Carbonic Anhydrase IX (CAIX). *J. Med. Chem.* **2017**, *60*, 9003–9011.

(25) Swain, B.; Angeli, A.; Singh, P.; Supuran, C. T.; Arifuddin, M. New Coumarin/Sulfocoumarin Linked Phenylacrylamides as Selective Transmembrane Carbonic Anhydrase Inhibitors: Synthesis and in-Vitro Biological Evaluation. *Bioorg. Med. Chem.* **2020**, *28*, No. 115586.

(26) Gualdani, R.; Ceruti, S.; Magni, G.; Merli, D.; Di, L.; Mannelli, C.; Francesconi, O.; Richichi, B.; la Marca, G.; Ghelardini, C.; Moncelli, M. R.; Nativi, C. Lipoic-Based TRPA1/TRPV1 Antagonist to Treat Orofacial Pain. *ACS Chem. Neurosci.* **2015**, *6*, 380–385.

(27) Suo, Y.; Wang, Z.; Zubcevic, L.; Hsu, A. L.; He, Q.; Borgnia, M. J.; Ji, R. R.; Lee, S. Y. Structural Insights into Electrophile Irritant Sensing by the Human TRPA1 Channel. *Neuron* **2020**, *105*, 882–894.e5.

(28) Zheng, X. Q.; Wu, Y.-h.; Huang, J.-f.; Wu, A. M. Neurophysiological Mechanisms of Cancer-Induced Bone Pain. *J. Adv. Res.* **2022**, *35*, 117–127.

(29) Schwab, A.; Stock, C. Ion Channels and Transporters in Tumour Cell Migration and Invasion. *Philos. Trans. R. Soc., B* **2014**, *369*, No. 20130102.

(30) Schwab, A.; Fabian, A.; Hanley, P. J.; Stock, C. Role of Ion Channels and Transporters in Cell Migration. *Physiol. Rev.* **2012**, *92*, 1865–1913.

(31) Berdiaki, A.; Datsis, G. A.; Nikitovic, D.; Tsatsakis, A.; Katonis, P.; Karamanos, N. K.; Tzanakakis, G. N. Parathyroid Hormone (PTH) Peptides through the Regulation of Hyaluronan Metabolism Affect Osteosarcoma Cell Migration. *IUBMB Life* **2010**, *62*, 377–386.

(32) Datsis, G. A.; Berdiaki, A.; Nikitovic, D.; Mytilineou, M.; Katonis, P.; Karamanos, N. K.; Tzanakakis, G. N. Parathyroid Hormone Affects the Fibroblast Growth Factor-Proteoglycan Signal-

ing Axis to Regulate Osteosarcoma Cell Migration. *FEBS Journal* **2011**, *278*, 3782–3792.

(33) Gkika, D.; Prevarskaya, N. Molecular Mechanisms of TRP Regulation in Tumor Growth and Metastasis. *Biochim. Biophys. Acta, Mol. Cell Res.* **2009**, *1793*, 953–958.

(34) Becchetti, A.; Arcangeli, A. Integrins and Ion Channels in Cell Migration: Implications for Neuronal Development, Wound Healing and Metastatic Spread. *Adv. Exp. Med. Biol.* **2010**, *674*, 107–123.

(35) Barry, E. L.; Gesek, F. A.; Froehner, S. C.; Friedman, P. A. Multiple Calcium Channel Transcripts in Rat Osteosarcoma Cells: Selective Activation of  $\alpha(1D)$  Isoform by Parathyroid Hormone. *Proc. Natl. Acad. Sci. U.S.A.* **1995**, *92*, 10914–10918.

(36) Devesa, I.; Planells-Cases, R.; Fernández-Ballester, G.; González-Ros, J. M.; Ferrer-Montiel, A.; Fernández-Carvajal, A. Role of the Transient Receptor Potential Vanilloid 1 in Inflammation and Sepsis. *J. Inflammation Res.* **2011**, *4*, 67–81.

(37) Diogenes, A.; Akopian, A. N.; Hargreaves, K. M. NGF Up-Regulates TRPA1: Implications for Orofacial Pain. *J. Dent. Res.* **2007**, *86*, 550–555.

(38) Ogawa, N.; Kawai, H.; Terashima, T.; Kojima, H.; Oka, K.; Chan, L.; Maegawa, H. Gene Therapy for Neuropathic Pain by Silencing of TNF- $\alpha$  Expression with Lentiviral Vectors Targeting the Dorsal Root Ganglion in Mice. *PLoS One* **2014**, *9*, No. e92073.

(39) Hadjicharalambous, C.; Kozlova, D.; Sokolova, V.; Epple, M.; Chatzinikolaïdou, M. Calcium Phosphate Nanoparticles Carrying BMP-7 Plasmid DNA Induce an Osteogenic Response in MC3T3-E1 Pre-Osteoblasts. *J. Biomed. Mater. Res., Part A* **2015**, *103*, 3834–3842.

## NOTE ADDED AFTER ASAP PUBLICATION

After this paper was published ASAP September 13, 2022, a label was corrected in the TOC/abstract graphic. The revised version was reposted October 10, 2022.

## Recommended by ACS

### Targeting Receptor-Interacting Protein Kinase 1 by Novel Benzothiazole Derivatives: Treatment of Acute Lung Injury through the Necroptosis Pathway

Xinqi Zhang, Chunlin Zhuang, *et al.*

MARCH 12, 2023

JOURNAL OF MEDICINAL CHEMISTRY

READ 

### Discovery and Characterization of the Topical Soft JAK Inhibitor CEE321 for Atopic Dermatitis

Gebhard Thoma, Hans-Guenter Zerwes, *et al.*

JANUARY 19, 2023

JOURNAL OF MEDICINAL CHEMISTRY

READ 

### Improvement of the Metabolic Stability of GPR88 Agonist RTI-13951-33: Design, Synthesis, and Biological Evaluation

Md Toufiquir Rahman, Chunyang Jin, *et al.*

FEBRUARY 07, 2023

JOURNAL OF MEDICINAL CHEMISTRY

READ 

### Evaluation of Broad Anti-Coronavirus Activity of Autophagy-Related Compounds Using Human Airway Organoids

Rina Hashimoto, Kazuo Takayama, *et al.*

MARCH 22, 2023

MOLECULAR PHARMACEUTICS

READ 

Get More Suggestions >